PERGAMON

International Journal of Heat and Mass Transfer 41 (1998) 4385–4392

International Journal of HEAT and MASS TRANSFER

Technical Note
Flow characteristics in a heated rotating straight pipe

M. A. Petrakis

Department of Physics, University of Patras, 26500 Patras, Greece

Received 23 October 1997; in final form 18 February 1998

Nomenclature

A function of r, θ
c pressure gradient
c_i coefficient ($i = 0, 1, 2, 3, 4$)
$c' = \alpha^3/\nu^2 c$
C_p specific heat
f dimensionless streamfunction
h, k grid size
g gravitational acceleration
m_i, m_i' coefficients ($i = 0, 1, 2, 3, 4$)
n_i, n_i' coefficients ($i = 0, 1, 2, 3, 4$)
Nu dimensionless Nusselt number
P_r Prandtl number
r, θ, z dimensionless cylindrical coordinates
R_a Rayleigh number
R_e Reynolds number based on the axial velocity
R_r Reynolds number based on the angular velocity
u, v, w dimensionless velocity components
W_m mean axial velocity.

Greek symbols
α radius of the pipe
β thermal expansion coefficient
$\varepsilon = R_e R_a R_r$
ζ dimensionless vorticity
Θ dimensionless temperature
κ diffusivity
λ the ratio h/k
ν kinematic viscosity
π radian
ρ fluid density
τ temperature gradient
τ_{ax} dimensionless axial shear stress
τ_{az} dimensionless azimuthal shear stress
ω relaxation factor
Ω angular velocity.

Subscripts/superscripts
0, 1, 2, 3, 4 position of the nodes on the computational domain
s loop counter.

Symbol
∇^2 dimensionless Laplacian operator.

1. Introduction

The flow in a rotating or in a heated straight pipe has been extensively studied not only for academic interest, but also for the great importance in mechanical applications such as in pipe heat exchangers, in cooling systems of rotor blades in gas turbines and in chemical mixing. The viscous flow in a straight pipe rotating about an axis perpendicular to its own, has as a result the generation of a secondary flow that is sustained by the Coriolis force introduced by the rotation of the pipe. Barua [1] used a regular perturbation about the Poiseuille flow limit, similar to Dean's [2, 3] approach for stationary and curved pipe flow. He showed that rotation generates a secondary flow and that it depends on the non-dimensional parameter $R_r = (2\Omega\alpha^2/\nu)$, where Ω is the angular frequency of rotation, α is the radius of the pipe and ν is the kinematic viscosity. Subsequent boundary-layer analysis also predicted a significant increase in the friction factor with rotational speed for small rotational rates and high axial pressure gradients (Mori and Nakayama [4], Ito and Nanbu [5]), the latter group also obtaining satisfactory agreement with their experimental results. Mansour [6] considered higher rotational velocities using a computer extension for the perturbation expansion, similar to a method that was applied by Van Dyke [7–

* Corresponding author.

PII: S0017–9310(98)00079–9

9] who studied the flow in a stationary straight pipe. According to this method the equations of motion are modified, so that they are depend on a single parameter $K = R_e R_r$, under the assumption that $R_e \to \infty$, $R_r \to 0$, where R_e is the Reynolds number based on the axial velocity. Benton [10] considered small rotational velocities and constructed a small perturbation expansion about the Hagen–Poisseuille flow. Later, Benton and Boyer [11] assumed the case of a rapid rotating conduit with $R_r R_e \leqslant 1$. Duck [12] used a numerical procedure, based on a combination of Fourier decomposition and finite difference discretization to study the flow structure in rotating circular ducts.

The first experiments concerning a rotating pipe were conducted by Trefethen [13] who observed that rotation transfers the onset of turbulence to higher Reynolds numbers. Later, Euteneuer and Piesche [14] in their experimental studies in circular pipes confirmed that the pressure drop is significantly higher than that for straight pipes, in agreement with the theoretical results.

The earliest analysis on the flow in a heated straight pipe was considered by Morton [15]. His study was restricted to small rates of heating and he obtained solutions for the axial velocity and temperature as power series depending on the parameters $R_e R_a$, where R_a is the Rayleigh number based on the temperature gradient along the pipe wall. Mori and Nakayama [16] assumed velocity and temperature boundary layers along the pipe wall and analysed theoretically the flow field and the temperature field. Van Dyke [17] modified Morton's variable in order to clarify the dependence of the problem on the parameters P_r, R_a and R_e, where P_r is the Prandtl number. The advantage of these simplifications was that the flow depended only on two parameters $\varepsilon = P_r R_a R_e$ and P_r, respectively. Guiasu et al. [18] were able to compute many terms of the series on Morton's problem using symbolic computation packages.

In the present work we study the fully developed steady flow in a straight rotating heated pipe with circular cross-section. The equations of motion and energy depend on three parameters that characterize the flow, the rotational Reynolds number R_r, the Reynolds number based on the axial flow R_e and the Rayleigh number R_a, and they are solved both analytically and numerically. In the analytical solution the functions of the flow are expanded in power series of the parameters R_r and R_a. Because of the difficulties of the problem introduced by the presence of these three parameters, we were able to compute only ten terms in each series, so that the range of values of the parameters for which the analytical solution converges is limited by the products $R_e R_a < 1000$ and $R_e R_r < 250$. However the analytic expression is of some value because it provides us with a mathematical expression showing the trend of the flow characteristics as well as with a benchmark for the numerical solution. In the numerical solution we consider a grid of mesh points in the circular domain and we modify the differential equations by approximating all partial derivatives with central differences. In this way we deduce an algebraic system of equations for all the points of the circular region that is solved using an iterative procedure. The limits of the products $R_e R_a$ and $R_e R_r$ for which the numerical solution is valid are $R_e R_a < 20\,000$ and $R_e R_r < 5000$. We compared the results obtained by the two methods and finally we examined the influence of Coriolis and buoyancy forces on the flow and the dependence of some properties of the flow, as the axial and azimuthal stresses, the Nusselt number, on the previous products.

2. Equations of motion and energy

A straight pipe of circular cross-section rotates in a horizontal plane about a vertical axis Oy, normal to its own. The temperature gradient along the axis Oz is constant. The geometry implies the use of a non-dimensional cylindrical coordinate system r, θ and z (Fig. 1). In this system let u, v and w be the corresponding velocity components and Ω the angular velocity. For an observer looking downward the pipe rotates in the counterclockwise direction. Let f and Θ be the non-dimensional streamfunction and fluid temperature, respectively. The equations of motion and energy for the steady state are

$$\nabla^4 f - \frac{1}{r}\frac{\partial(f,\nabla^2 f)}{\partial(r,\theta)} = R_r R_e\left(\frac{1}{r}\frac{\partial w}{\partial \theta}\sin\theta - \frac{\partial w}{\partial r}\cos\theta\right) + R_a\left(\frac{\partial \Theta}{\partial r}\sin\theta + \frac{1}{r}\frac{\partial \Theta}{\partial \theta}\cos\theta\right) \tag{1}$$

$$\nabla^2 w - \frac{1}{r}v\frac{\partial w}{\partial \theta} - u\frac{\partial w}{\partial r} = c' + \frac{R_r}{R_e}(v\cos\theta + u\sin\theta) \tag{2}$$

$$\nabla^2 \Theta - P_r\left(\frac{1}{r}v\frac{\partial \Theta}{\partial \theta} + u\frac{\partial \Theta}{\partial r}\right) = -R_e w \tag{3}$$

where

$$u = -\frac{1}{r}\frac{\partial f}{\partial \theta}, \quad v = \frac{\partial f}{\partial r}, \quad \nabla^2 = \frac{\partial^2}{\partial r^2} + \frac{1}{r}\frac{\partial}{\partial r} + \frac{1}{r^2}\frac{\partial^2}{\partial \theta^2} \tag{4}$$

and R_a is the Rayleigh number, R_r is the Reynolds number based on the rotation, R_e is the Reynolds number based on the mean axial velocity and P_r is the Prandtl number. The preceding nondimensional numbers of the flow are defined as follows

$$R_a = \frac{\beta g \alpha^4}{\nu^2} P_r, \quad R_e = \frac{W_m \alpha}{\nu}, \quad R_r = \frac{2\Omega\alpha^2}{\nu}, \quad P_r = \frac{\nu \rho C_p}{\kappa}$$

where ν is the kinematic viscosity, ρ is the fluid density, C_p is the specific heat, g is the gravitational acceleration,

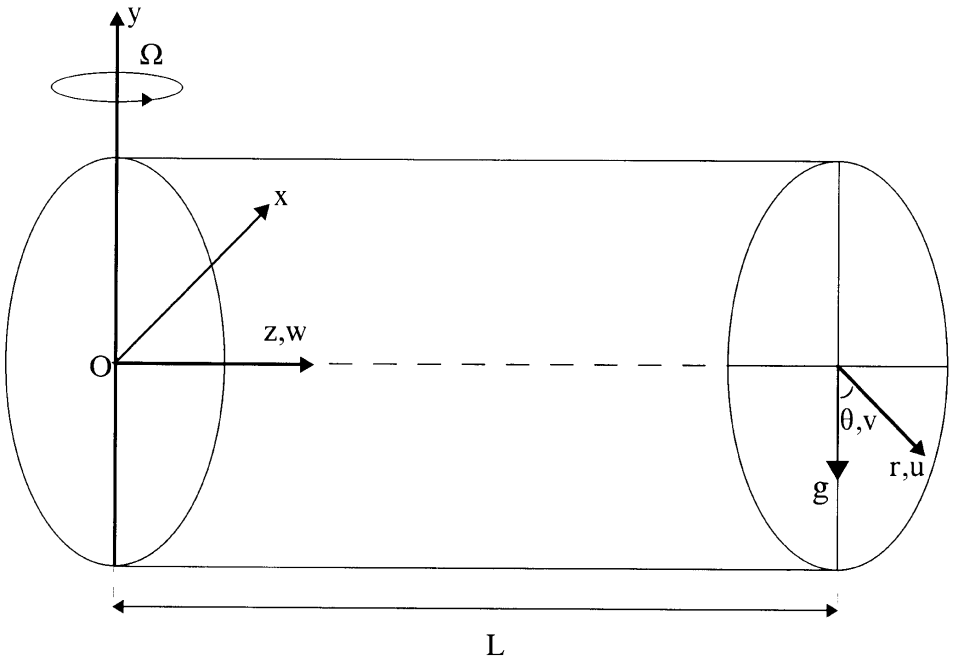

Fig. 1. Cylindrical coordinate system.

β is the thermal expansion coefficient, τ is the temperature gradient along the axis of the pipe, W_m is the mean velocity and κ is the diffusivity. The Boussinesq form has been employed in the preceding equations of motion to approximate the buoyancy forces.

The boundary conditions are $f = (\partial f/\partial r) = w = \Theta = 0$ at $r = 1$, whereas f, w and Θ are finite at $r = 0$.

3. Methods of solution

Equations (1)–(3) have been solved analytically and/or numerically. For the analytic solution we assume that each of the variables f, w and Θ can be expanded in a power series of the form

$$\begin{aligned} w &= w_{00} + R_r w_{10} + R_a w_{11} + R_r^2 w_{20} + R_a^2 w_{21} + R_r R_a w_{22} \\ &\quad + R_r^3 w_{30} + R_a^3 w_{31} + R_r^2 R_a w_{32} + R_r R_a^2 w_{33} + \cdots \\ f &= R_r f_{10} + R_a f_{11} + R_r^2 f_{20} + R_a^2 f_{21} + R_r R_a f_{22} + R_r^3 f_{30} \\ &\quad + R_a^3 f_{31} + R_r^2 R_a f_{32} + R_r R_a^2 f_{33} + \cdots \\ \Theta &= \Theta_{00} + R_r \Theta_{10} + R_a \Theta_{11} + R_r^2 \Theta_{20} + R_a^2 \Theta_{21} + R_r R_a \Theta_{22} \\ &\quad + R_r^3 \Theta_{30} + R_a^3 \Theta_{31} \\ &\quad + R_r^2 R_a \Theta_{32} + R_r R_a^2 \Theta_{33} + \cdots . \end{aligned} \tag{5}$$

In this way equations (1)–(3) are split in a number of differential equations that are solved analytically. The present analysis is carried out up to $R_e R_a \leqslant 1000$ and $R_e R_r \leqslant 250$. Of these limits the first has been set by Morton [15] and has been verified by Yao and Berger [19] and Karahalios [20]. The second has been established by Ito and Motai [21]. Comparison of the results of the analytic method with the corresponding results of the numerical method, that follows, shows that it fails to converge for values of these products greater than those already set.

The numerical method consists of the following steps.

The circular region $0 \leqslant r \leqslant 1$, $0 \leqslant \theta \leqslant 2\pi$ (Fig. 2) is divided into a grid formed by the radial lines $\theta = jk$ and the circles $r = ih$, where h, k denote the size of the grid in the increasing radial and angular direction, respectively. Let (r, θ) be a typical grid point. We denote (r, θ) by (r_0, θ_0). Adopting the Southwell notation all quantities at the point (r_0, θ_0) and the neighbouring points (r_0+h, θ_0), (r_0, θ_0+k), (r_0-h, θ_0) and (r_0, θ_0-k) are denoted by the subscripts 0, 1, 2, 3 and 4, respectively. Introducing the vorticity ζ, equation (1) takes the following form

$$\nabla^2 f = -\zeta \tag{6}$$

$$\nabla^2 \zeta - \frac{1}{r} v \frac{\partial \zeta}{\partial \theta} - u \frac{\partial \zeta}{\partial r} = -R_r R_e \left(\frac{1}{r} \frac{\partial w}{\partial \theta} \sin\theta - \frac{\partial w}{\partial r} \cos\theta \right) - R_a \left(\frac{1}{r} \frac{\partial \Theta}{\partial \theta} \cos\theta + \frac{\partial \Theta}{\partial r} \sin\theta \right) \tag{7}$$

whereas the other two (2)–(3) remain unaltered.

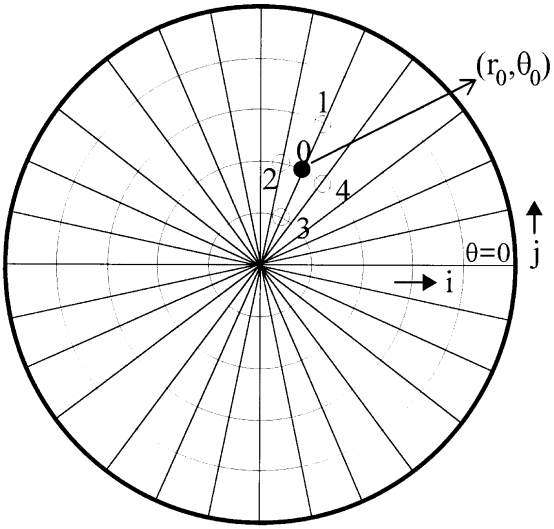

Fig. 2. Mesh points in r–θ plane.

In the next we give a brief description of the numerical method, solving equation (3). We separate equation (3), into two equations, namely

$$\frac{\partial^2\Theta}{\partial r^2}+\frac{P_r}{r}\frac{\partial\Theta}{\partial r}-P_r u\frac{\partial\Theta}{\partial r}=A(r,\theta)-R_e w$$

$$\frac{\partial^2\Theta}{\partial\theta^2}-rvP_r\frac{\partial\Theta}{\partial\theta}=-r^2A(r,\theta),$$

in which $A(r,\theta)$ is an unknown function. After lengthy manipulations (Petrakis and Karahalios [22]) we derive the following equation

$$n_1\Theta_1+n_2\Theta_2+n_3\Theta_3+n_4\Theta_4-n_0\Theta_0+h^2R_e w_0=0 \qquad (8)$$

where

$$n_1=1+\frac{P_r h}{2r_0}-\frac{P_r u_0 h}{2}+\frac{P_r^2u_0^2h^2}{8},$$

$$n_2=\lambda^2\left(\frac{1}{r_0^2}-\frac{P_r v_0 k}{2r_0}+\frac{P_r^2v_0^2}{8}\right)$$

$$n_3=1-\frac{P_r h}{2r_0}+\frac{P_r u_0 h}{2}+\frac{P_r^2u_0^2h^2}{8},$$

$$n_4=\lambda^2\left(\frac{1}{r_0^2}+\frac{P_r v_0 k}{2r_0}+\frac{P_r^2v_0^2}{8}\right)$$

$$n_0=2+\frac{2\lambda^2}{r_0^2}+\frac{P_r^2h^2}{4}(u_0^2+v_0^2),$$

$$u_0=\frac{f_2-f_4}{2kr_0},\quad v_0=-\frac{f_1-f_3}{2h},\quad \text{and}\quad \lambda=h/k. \qquad (9)$$

Equation (8) holds at all grid points for which $0<r<1$. The matrix associated with (8) is diagonally dominant. In this way we obtain approximations to the values of Θ at all grid points in the domain $0<r<1$, $0\leqslant\theta<2\pi$. The boundary conditions are that the temperature is zero at $r=1$ and finite at $r=0$. The truncation error in (8) is $O(h^4)+O(h^2k^2)$. It should be noted here that the conditions at the centre of the pipe cannot be fulfilled with the use of the preceding system of equations. Hence we consider a Cartesian coordinate system (Fig. 3) with origin at the centre of the circular cross-section. In this system equation (3) takes the form

$$n_1'\Theta_1+n_2'\Theta_2+n_3'\Theta_3+n_4'\Theta_4-n_0'\Theta_0+h^2R_e w_0=0 \qquad (10)$$

where

$$n_1'=1-\frac{P_r u_0 h}{2}+\frac{P_r^2u_0^2h^2}{8},$$

$$n_2'=1-\frac{P_r v_0 h}{2}+\frac{P_r^2v_0^2h^2}{8}$$

$$n_3'=1+\frac{P_r u_0 h}{2}+\frac{P_r^2u_0^2h^2}{8},$$

$$n_4'=1+\frac{P_r v_0 h}{2}+\frac{P_r^2v_0^2h^2}{8}$$

$$n_0'=4+\frac{P_r^2h^2}{4}(u_0^2+v_0^2),$$

$$u_0=\frac{f_2-f_4}{2h}\quad\text{and}\quad v_0=-\frac{f_1-f_3}{2h}. \qquad (11)$$

In a similar way we deduce analogous equations to approximate equations (2), (6) and (7) at all grid points within the domain $0<r<1$, $0\leqslant\theta<2\pi$. In order to solve numerically the previous finite-difference equations we employ the S.O.R. method repeating the iterative procedure until the adopted criterion of accuracy for each one of them is satisfied. For Θ_0 we have adopted that

$$\max\left|1-\frac{\Theta_0^{(s)}}{\Theta_0^{(s+1)}}\right|\leqslant 10^{-5}$$

and the same is valid for the other variables w_0, ζ_0 and f_0.

Once all quantities have converged to limits, the iterative sequence is terminated. In this way the numerical procedure converges for a large range of values of the parameters R_r, R_a and R_e. In particular, the accuracy of the numerical solution is limited by the values of the products $R_eR_r\leqslant 5000$ and $R_eR_a\leqslant 20\,000$ with $R_r<30$, $R_a<80$ and $R_e<5000$. The value of the Prandtl number for which our results obtained is equal to unity.

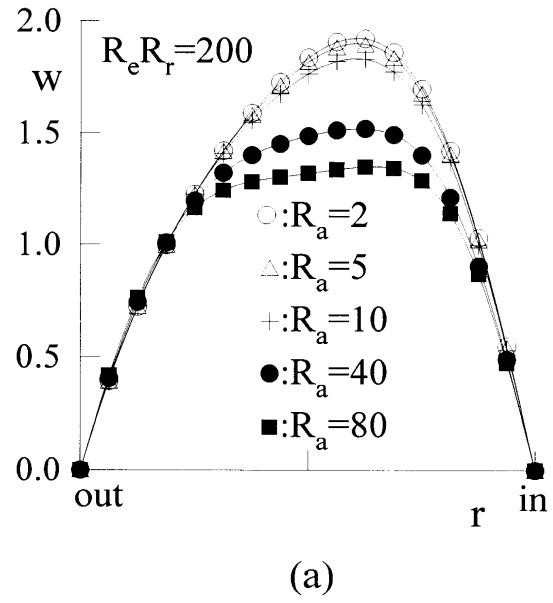

(a)

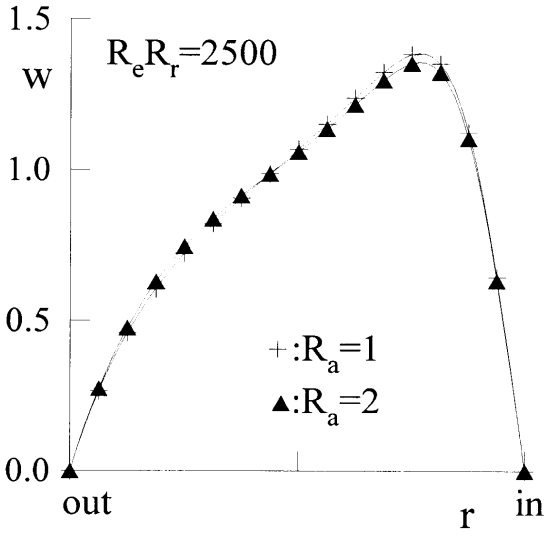

(b)

Fig. 3. Axial velocity profile along the horizontal diameter.

4. Results and discussion

In the next all graphs are based on the numerical solution, unless it is otherwise stated. In Fig. 3 we show the variation of the axial velocity profile w with r along the horizontal diameter of the pipe for various values of the product R_eR_r and for Rayleigh number varying between $R_a = 1$ and $R_a = 80$. For $R_eR_r < 200$ and for small values of R_a ($R_a = 2, 5, 10$) (Fig. 3a) the curves are nearly parabolic and like those in the classical solution of the Hagen–Poisseuille flow. As R_a increases, the maximum of the axial velocity reduces to lower values and the curves become more flat. This is explained by the fact that the axial induced by the temperature gradient opposes the axial flow due to the pressure gradient. Hence an increase in R_a causes decrease in w. When R_eR_r takes larger values and R_a varies (Fig. 3b) the axial velocity curved become again flat. In this case a thin boundary layer is formed on the inner side in agreement to Benton and Boyer [11]. It is realized that the variation of the Rayleigh number does not affect the form of the axial velocity profile. In Fig. 4 we make a comparison between the results of the two methods, the analytical and the numerical, respectively. As it is seen, for $R_eR_r = 200$ and $R_a = 5$, the results of the analytical solution are in good agreement with those of the numerical solution. As the values of R_e, R_a and R_r increase the analytical solution fails to converge. The limits of the values of the parameters for which the results of the analytical solution are acceptable are $R_eR_r < 250$ and $R_eR_a < 1000$. The first limit has been also established by Ito and Motai [21] and the second by Morton [15]. The axial shear stress $\tau_{ax} \propto (\partial w/\partial r)_{r=1}$ along the pipe wall is plotted in Fig. 5 for $R_eR_r = 3000$ and R_a varying between the values $R_a = 1$ and $R_a = 5$. We see that the variation of the Rayleigh number R_a does not seriously affect the values and the position of maximum of the axial shear stress. This is so because for such

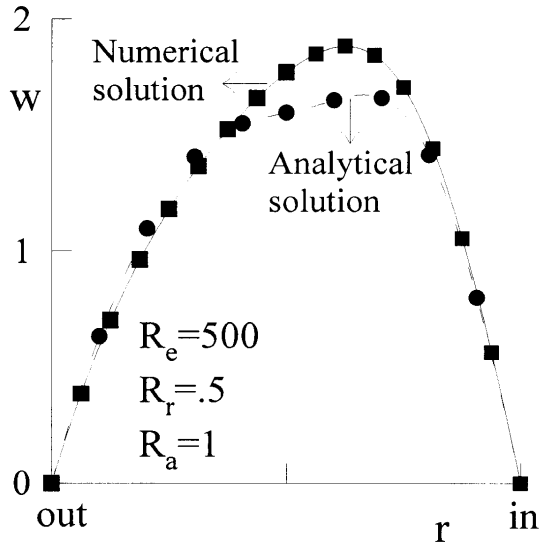

Fig. 4. Comparison between the analytical and the numerical solution.

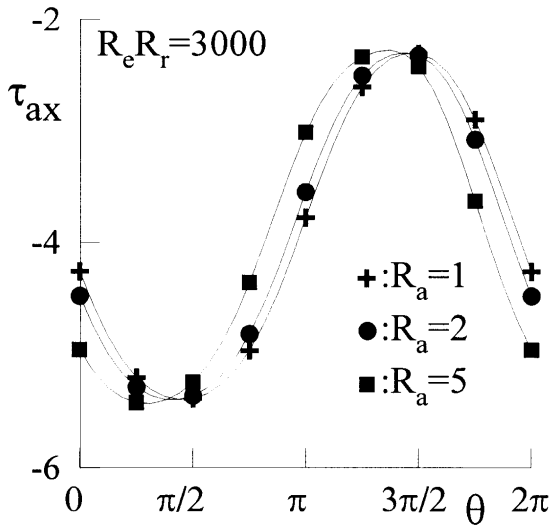

Fig. 5. Axial shear stress along the pipe wall.

large values of R_eR_r and within the limits of the present numerical solution the axial velocity profiles remain unaffected by the variation of the Rayleigh number, as it is realized by Fig. 3b.

In Fig. 6 we show the secondary flow pattern and the isovelocity curves for $R_e = 100$ (Fig. 6a, b) and $R_e = 5000$ (Fig. 6c). Figure 6a, b refer to the same Rayleigh number $R_a = 80$ but to different rotational Reynolds numbers ($R_r = 1, 30$) so that the effect of Coriolis forces on the axial and on the secondary flow will be illustrated. It is known that in the absence of heat the secondary flow streamlines are symmetric with respect to the horizontal diameter of the pipe and in the main core of the fluid they run along this diameter. In addition, these streamlines tend to accumulate to that side of the wall toward which the Coriolis force points, when the frequency of rotation increases. On the other hand, in the case of no rotation, the secondary flow streamlines are symmetric with respect to the vertical diameter. In both cases the isovelocity contours are circles concentric to the pipe. In Fig. 6a we show the effect of a weak rotation on the secondary flow. The streamlines still remain symmetric to the vertical diameter of the pipe. Increase in the value of the rotational number (Fig. 6b) turns the flow field so that the dividing streamline becomes nearly horizontal. It is therefore concluded that a large frequency of rotation tends to restore the secondary flow pattern to the state of straight rotating pipe and nearly cancels the heating effects. This is shown in Fig. 6c. In addition the secondary flow becomes faster. This is attributed to the mutual effect of each force. Since the Coriolis force and the buoyancy force generate independently a secondary motion, the two motions enhance each other and eventually result in a stronger rotational flow. It is worthy to note that for these large products R_eR_r and R_eR_a the dividing streamline does not pass through the centre of the pipe, neither is straight anymore. With respect to the axial velocity contours it is seen that an increased Rayleigh number displaces its maximum downward whereas for high Reynolds number R_r the maximum is driven along the direction of the Coriolis force. Conclusively, we observe that a strong secondary flow may occur when either R_r is large and R_a is small or when R_r is small and R_a is large. In both cases a strong secondary flow increases the viscous shearing stresses and, as a result, the axial velocity falls to lower values. In Fig. 7 we examine the effect of the parameters R_a and R_r on the azimuthal shear stress $\tau_{az} \propto (\partial^2 f/\partial r^2)_{r=1}$ on the pipe wall. Increase either in the frequency of rotation or in the temperature gradient, induces a relatively strong secondary flow and accordingly an increased azimuthal shear stress.

The temperature profile along the horizontal diameter is presented in Fig. 8 for $R_e = 5000$. It is seen that, in general, the temperature distribution follows the form of the axial velocity, a property that also holds for isothermal curves. Finally, in Fig. 9 we have plotted the variation of the Nusselt number $Nu = (\partial\Theta/\partial r)_{r=1}$ on the pipe wall for $R_eR_r = 3000$ and R_a varying. When the product R_eR_a is small ($R_eR_a = 3000$, 6000) the form of the curves remains unaffected, whereas for $R_eR_a = 15\,000$ the maximum and the minimum of the Nusselt number is slightly displaced to smaller angles. This is because the bulk of the heat flux is conveyed by the axially moving fluid.

5. Conclusions

The steady flow and heat transfer is investigated in a rotating straight pipe. The effects of Coriolis and buoyancy forces on the flow structure and on the flow properties are studied. The obtained results are summarized as follows:

(1) The analytical solution fails to converge for values of the products R_eR_r and R_eR_a greater than the values 250 and 1000, respectively, whereas the corresponding values for the numerical solution are 5000 and 20 000. In addition the present numerical solution holds for $R_r < 30$, $R_a < 80$ and $R_e < 5000$.
(2) The flow field and the temperature distribution are affected by the rotation of the pipe and the heat and are dependent on the values of the products R_eR_r and R_eR_a, respectively.
(3) The flow properties, such as the shear stresses and the Nusselt number, depend on the values of the products R_eR_r and R_eR_a, respectively. However, their variation is not significant when R_eR_a increases.

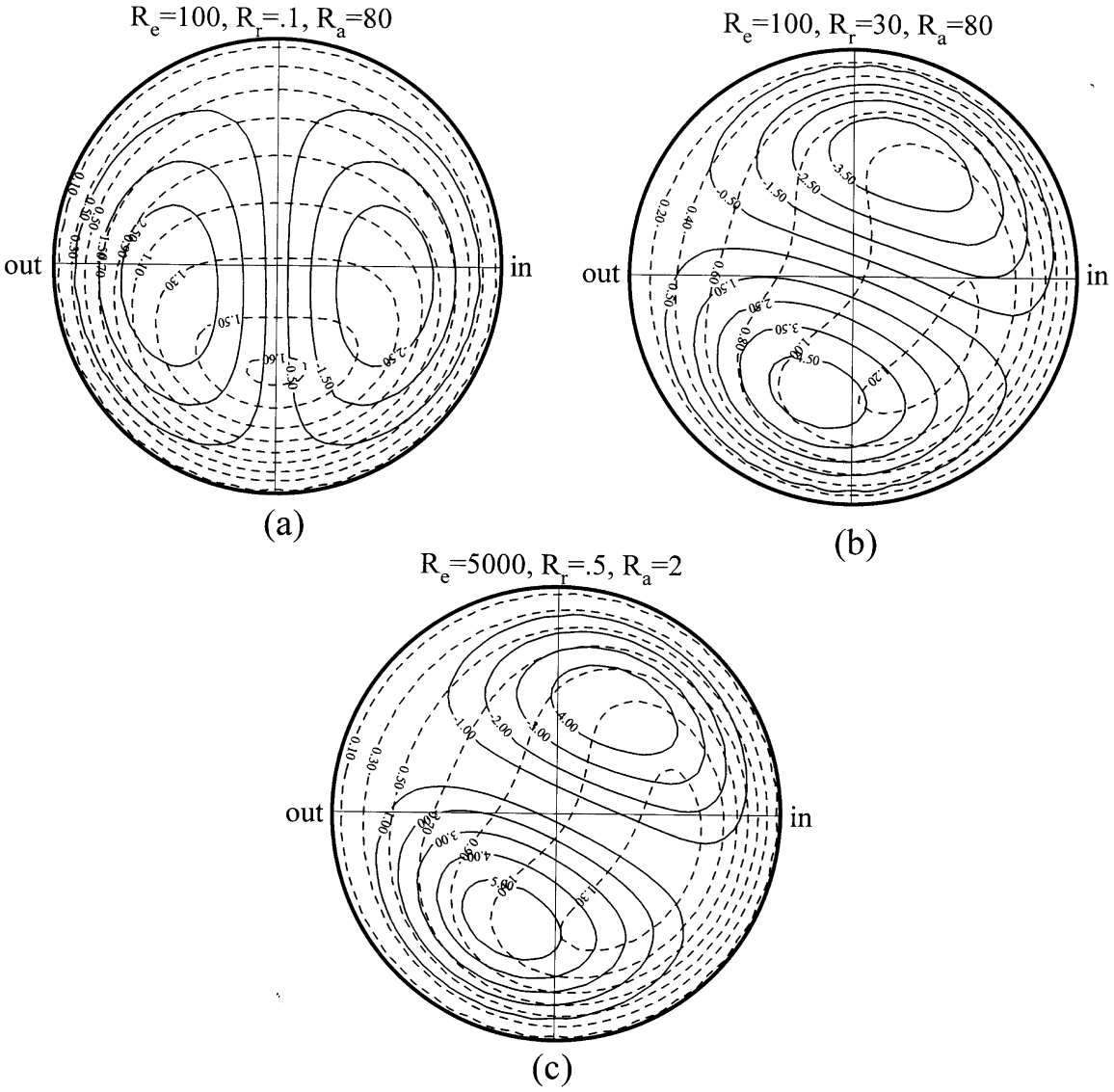

Fig. 6. Secondary flow pattern and isovelocity contours.

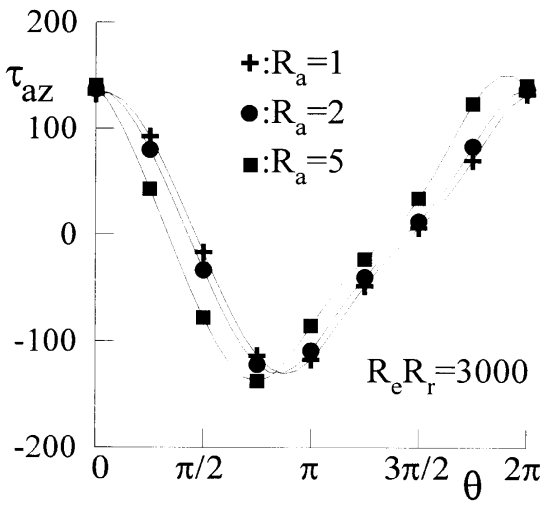

Fig. 7. Azimuthal shear stress on the pipe wall.

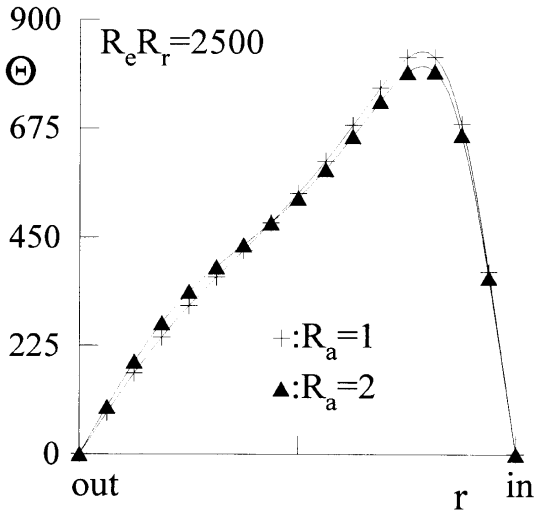

Fig. 8. Temperature distribution along the horizontal diameter.

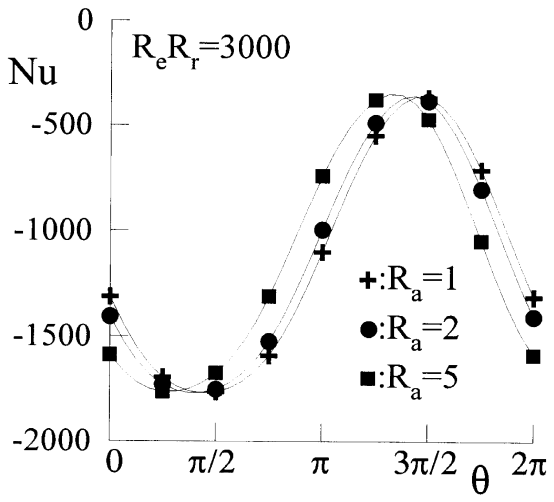

Fig. 9. Variation of the Nusselt number on the pipe wall.

References

[1] S.N. Barua, Secondary flow in a rotating straight pipe, Proceedings of the Royal Society of London A 227 (1954) 133–139.

[2] W.R. Dean, Note on the motion of fluid in a curved pipe, Philosophical Magazine 4 (1927) 208–223.

[3] W.R. Dean, The streamline motion of fluid in a curved pipe, Philosophical Magazine 5 (1928) 673–695.

[4] Y. Mori, W. Nakayama, Forced convective heat transfer in a straight pipe rotating about a parallel axis (1st Report, Laminar region). International Journal of Heat and Mass Transfer 10 (1967) 1179–1194.

[5] H. Ito, K. Nanbu, Flow in rotating straight pipes of circular cross-section, J. Basic Engng Trans ASME D 93 (1971) 383–394.

[6] K. Mansour, Laminar flow through a slowly rotating straight pipe, Journal of Fluid Mechanics 150 (1985) 1–21.

[7] M. Van Dyke, Extended Stokes series: laminar flow through a loosely coiled pipe, Journal of Fluid Mechanics 86 (1978) 129–145.

[8] M. Van Dyke, Analysis and improvement of perturbation series, Q. J. Mech. Appl. Maths 27 (1974) 423–450.

[9] M. Van Dyke, Computer extension of perturbation series in fluid mechanics, SIAM Journal of Applied Mathematics 28 (1975) 720–734.

[10] G.S. Benton, The effects of the earth's rotation on laminar flow in pipes, Journal of Applied Mechanics 23 (1956) 123–127.

[11] G.S. Benton, D. Boyer, Flow through a rapidly rotating conduit of arbitrary cross-section, Journal of Fluid Mechanics 26 (1966) 69–79.

[12] P. Duck, Flow through rotating straight pipes of a circular cross-section, Physics of Fluids 26 (1983) 614–618.

[13] L. Trefethen, Fluid flow in radial rotating tubes, in: Actes, 9eme Congr. Intle de Mec. Appl. 1 (1957) 341–350.

[14] G.A. Euteneuer, M. Piesche, Druckabfallmessungen in stationar rotierenden, gekrummten kanalstrecken mit quadratischem sowie kreisformigen Durchflubquerschnitt, Forsch. Ing.-Wes. 44 (1978) 53–56.

[15] B.R. Morton, Laminar convection in uniformly heated horizontal pipes at low Rayleigh number, Q. J. Mech. Appl. Maths 12 (1959) 410–420.

[16] Y. Mori, W. Nakayama, Study on forced convective heat transfer in curved pipes (1st Report, Laminar region), International Journal of Heat and Mass Transfer 8 (1965) 67–82.

[17] M. Van Dyke, Extended Stokes series: laminar flow through a heated horizontal pipe, Journal of Fluid Mechanics 212 (1990) 289–308.

[18] I. Guiasu, H. Raszillier, K. Nandakumar, Laminar convection in a uniformly heated horizontal pipe using symbolic computation, Comp. Fluid Dyn. 3 (1994) 193–216.

[19] L.S. Yao, S.A. Berger, Flow in heated curved pipes. Journal of Fluid Mechanics 88 (1978) 339–354.

[20] G.T. Karahalios, Mixed convection flow in a heated curved pipe with core, Physics of Fluids A 2 (1990) 2164–2175.

[21] H. Ito, T. Motai, Secondary flow in a rotating curved pipe, Rep. Inst. High Speed Mech. 29 (1974) 33–57.

[22] M.A. Petrakis, G.T. Karahalios, Steady flow in a curved pipe with a coaxial core, International Journal for Numerical Methods in Fluids 22 (1996) 1231–1237.